TABLE I. Comparison of Wall Thickness in Biotubes Before and After Implantation and Native Arteries

		Wall Thickness (μm)
Native		189.1 ± 22.6
Biotube	Caff portion	127.3 ± 22.2
	Anastomosis portion	211.9 ± 24.1
	Midportion	149.5 ± 13.8

endogenous peroxidase and then incubated overnight with the primary antibody at 4°C. After treatment with biotinylated secondary antibodies (LSAB system, Dako Japan), the sections were incubated with peroxidase-conjugated streptavidin for 30 min. Finally, visualization was carried out by treatment with 0.02% 3,3′-diaminobenzidine tetrahydrochloride (DAB) in 0.05 mol/L Tris-HCl buffer containing 0.005% H_2O_2 for 5 min. All stained sections were observed using light or polarizing microscopy.

Mechanical properties

Mechanical properties of the biotubes ($n = 5$ before implantation, $n = 1$ after implantation) and native carotid arteries ($n = 5$) were examined using a tensile tester (RE-3305, Yamaden, Tokyo, Japan). Tubular samples were cut circumferentially and opened. Tissue specimens 3 mm in width and 9 mm in length were tested under humid conditions. The load was recorded until the samples ruptured under a tissue-extension rate of 50 μm/s. Elastic modulus values were obtained from the deformation-force relationships.

Statistics

Results are expressed as mean ± standard error of the mean. An unpaired t test (Student's t test) was performed.

RESULTS

Biotube implantation

Biotubes ($n = 6$) with reinforced ends were prepared according to the previously reported method[4] by embedding the specially designed mold—a silicone rod (diameter, 3 mm; length, 30 mm) tightly covered at both ends with two pieces of short polyurethane sponge tubes—into the dorsal subcutaneous pouches of two rabbits for 2 months. The resulting biotubes were completely encapsulated by very thin homogeneous autologous connective tissues (wall thickness, 76 ± 37 μm).

One biotube was autoimplanted in the carotid artery of a rabbit by means of an end-to-end anastomosis between divided native arteries with little excision [Figure 1(A)]. During surgery, no major discrepancies were observed between the sponge regions of the biotube and the ends of the native artery to which the biotubes were anastomosed. After anastomosis was completed and blood circulation was reestablished, periodic cycles of inflation and deflation of the biotube were noted, indicating pulsatile blood flow in the implanted biotube. No instances of rupture or elongation occurred at the time of implantation.

Angiographic examination revealed that no aneurysms or stenoses had formed in the biotube at 17 months after implantation, although a large curvature in the artery shape was observed [Figure 1(C)]. The curvature observed in the artery was similar to that observed at 26 months after implantation [Figure 1(D)]. There were no aneurysms or stenoses even at 26 months. Figure 1(B) shows a macroscopic view of the biotube at 26 months after implantation. The biotube was easily harvested with minimal damage since there were few adhesions between the biotube tissue and the surrounding subcutaneous tissue [Figure 1(B)]. The shape of the biotube was very similar to that observed in angiography.

Macroscopic observation of the distal half of the harvested biotube revealed an extremely flat luminal surface including the anastomosis portion with the cuff sponge, which was completely impregnated into the vascular tissue [Figure 2(A)]. Minimal thrombus formation and neointimal hyperplasia were observed on the biotube surface.

Histological change after implantation

The wall thickness of the harvested biotube was almost uniform all around [Figure 2(B)]. No abnormal collection or infiltration of inflammatory cells was observed in the wall. Because the wall structure was also almost uniform, it was very difficult to distinguish between the biotube tissue before implantation and the developed neointimal tissue; in fact, it was suspected that the biotube tissue was replaced with the formed neointimal tissue. The all-over wall thickness was 127 ± 22 μm at the proximal cuff portion, 212 ± 24 μm at the proximal anastomosis portion, and 150 ± 14 μm at the midportion (Table I). Even at 26 months after implantation, no significant neointimal thickening was observed. The thickness was similar to those at the midportion of the biotubes at 1.5 months of implantation (217 ± 37 μm) or 3 months (170 ± 30 μm). In addition, all of the biotube thicknesses were very close to those of the native carotid arteries (189 ± 23 μm).

On the other hand, interestingly, the reinforcement cuff, which was completely impregnated in the prepared biotube, was extracted from the biotube wall to its outer side at 26 months after implantation, indicating that no artificial material was included in the newly developed biotubes [Figure 2(C)]. Therefore, the anastomosis portion could not be indicated exactly in the hematoxylin–eosin stained tissue.

The entire luminal surface was completely covered with PECAM-1-positive endothelial cells from the proximal anastomosis portion [Figure 2(D)] to the midportion [Figure 2(E)], which was already observed at 3 months after implantation. Almost the entire luminal surface had a lamina elastica interna-like elastin layer [Figure 2(F)], whereas the anastomosis portion had a multilayered elastin network [Figure 2(G)]. The main component of the extracellular matrix was dense collagen, as in the prepared biotubes [Figure 3(A,D)]. However, the collagen was highly oriented in a circumferential manner [Figure 3(B,E)] as opposed to a random arrangement as before implantation. SMA-positive, that is, either myofibroblasts or smooth muscle cells surrounded the exit hole of the developed tissue and were highly oriented in a circumferential manner [Figure 3(C,F)]. The vascular wall structure was almost completely constructed.

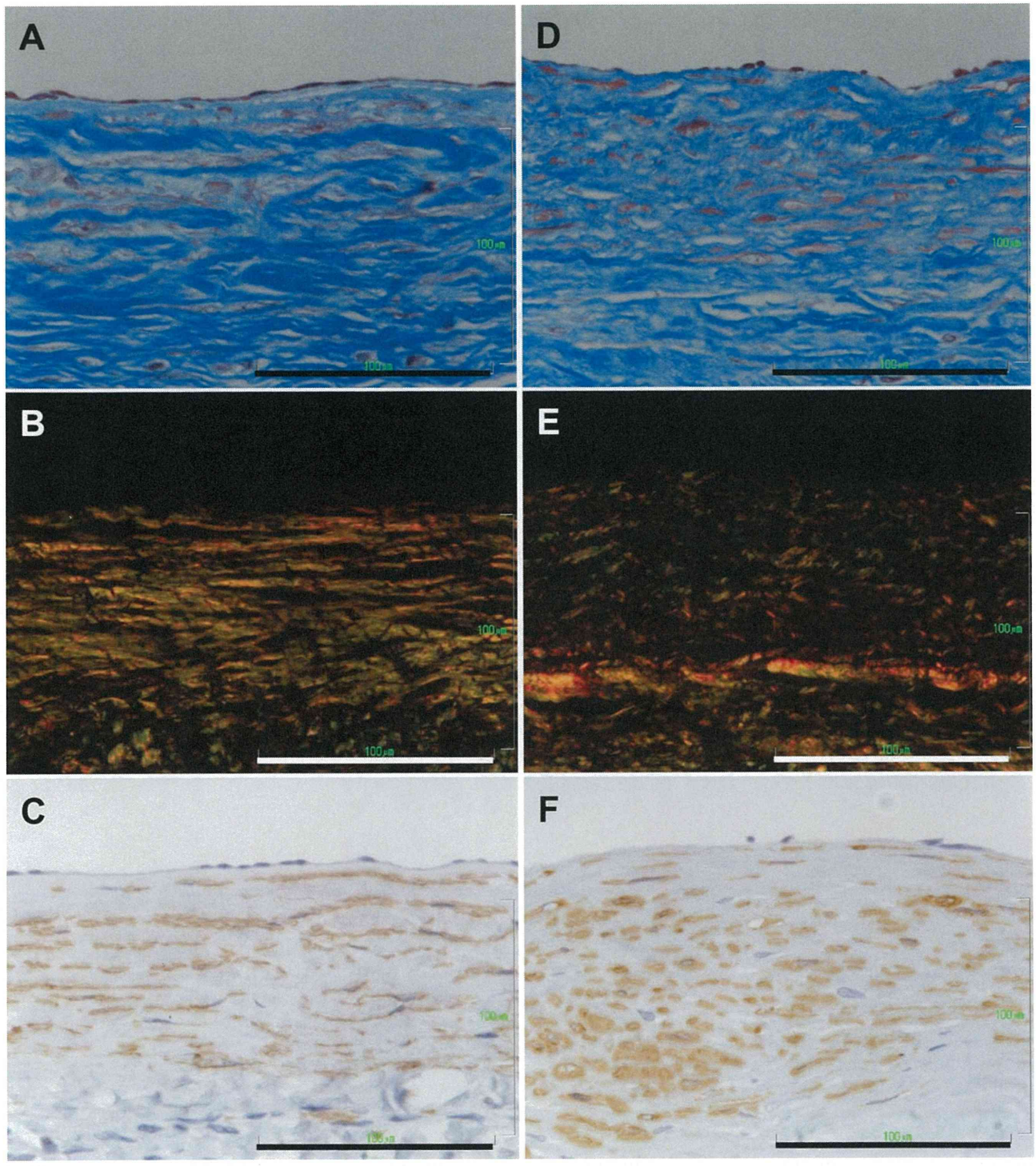

FIGURE 3. Histological photographs of the harvested biotube at the midportion stained with Masson's Trichrome (A and D), Sirius red observed through a polarizing microscope (B and E), and α-SMA immunohistologically (C and F) at the circumferential direction (A–C) and the longitudinal direction (D–F). Bar = 100 μm. [Color figure can be viewed in the online issue, which is available at wileyonlinelibrary.com.]

Mechanical changes after implantation

The tissue samples were obtained circumferentially. Ultimate strain, ultimate load, and elastic modulus values were obtained from the load-deformation relationships, which were obtained by circumferential elongation of the native arteries, and biotubes before and after implantation. All samples were ruptured at a similar strain range [Figure 4(A), native: 0.62 ± 0.12, $n = 5$; biotube before implantation: 0.50 ± 0.11, $n = 5$; after implantation: 0.69, $n = 1$]. However, the ultimate load equivalent to elongation strength of the biotube considerably increased from about half of the native strength before implantation to about twice that of the native

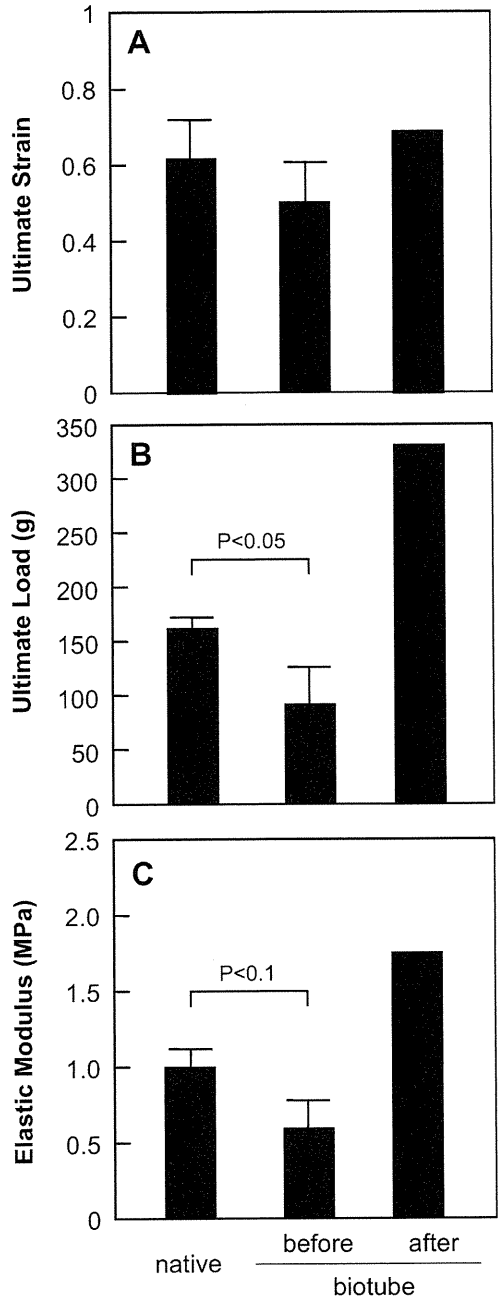

FIGURE 4. Comparison of the mechanical properties (A: ultimate strain; B: ultimate load; and C: elastic modulus) of the biotubes before ($n = 5$) and after implantation ($n = 1$) and those of the native arteries ($n = 5$).

strength after implantation [Figure 4(B)]. Therefore, the elastic modulus value of the biotube after implantation was 2× higher than that of the native arteries [Figure 4(C), native: 1.02 ± 0.18 MPa; biotube after implantation: 1.87 MPa]. The biotube after implantation acquired a robust property of maintenance of the preimplantation elongation ability.

DISCUSSION

This study was the first to show the *in vivo* structural and mechanical changes in long-term autoimplantation of a small-caliber, biotube vascular graft[3–5] with 3-mm diameter prepared by in-body tissue architecture technology. Although the sample number was extremely limited, both invaluable and informative results were obtained, which indicated the possible uses of biotube vascular grafts based on patency for implantation longer than 2 years.

Anastomosis between the biotube and the native artery could be easily performed in a conventional microsurgery using a cuff-impregnating technique.[4] In this study, the biotube was implanted by means of end-to-end anastomosis between divided native arteries with little excision to avoid mechanical stretching of the cuffs attached at the both ends of the biotube. As a result, a large arterial curvature was induced after implantation. During macroscopic observation of the biotube harvesting, a large winding section of artery in which the biotube was implanted was observed. This confirmed that the biotube had excellent flexibility despite the winding and did not fold. The high antithrombogenic potential of the biotube in the chronic phase was additionally suggested by its ability to withstand random blood flow in the winding vasculature. Because the biotube had adequate mechanical strength (about half that of the native artery) and high burst strength (~ 1000 mmHg), implantation under a stretching condition may be also feasible.

In our previous study on animal implantation of biotubes up to 3 months, high total patency of 9/11 without any instance of aneurysm or rupture was observed.[5] The wall thickness at the midportion of the biotubes was saturated at about 200 μm, 1.5 months after implantation. The wall thickness at 26 months of implantation in this study was about 150 μm at the midportion and about 200 μm even at the anastomosis portion. Thin wall thickness similar to that of the native artery (~ 200 μm) was maintained even during the chronic stage.

The concept of tissue engineering using biodegradable materials was proposed about 20 years ago,[9] and such materials were previously developed and a part of them clinically applied with autologous cell seeding or bioreactor culturing.[10–13] However, the usefulness of these materials for reconstruction of small-caliber vascular grafts has been demonstrated. On the other hand, interestingly, the cuff materials used for anastomosis reinforcement, which was uniform in the prepared biotubes, were completely excised from the biotube in this study. The reconstructed vascular wall contained only completely autologous tissue without any artificial material. Therefore, we strongly believe that the implanted biotube will adapt as the recipient grows.

In previous histological examination,[3] before implantation, biotube wall was composed of collagen-rich tissue and no elastic fibers. No abnormal collection or infiltration of inflammatory cells was observed. In addition, immunohistochemical staining showed that almost all cells in the wall were fibroblasts. At 3 months after implantation, collagen fibers were oriented in a circumferential manner as opposed to their random arrangement before implantation.[5] α-SMA-positive cells, that is, either myofibroblasts or smooth muscle cells, were accumulated on the luminal surface of the biotube. PECAM-1-positive endothelial cells completely covered the luminal surface. In addition, a few elastic fibers were

produced. Histological changes in the biotube tissue that occurred between 3 and 26 months after implantation were the orientation of α-SMA-positive cells and the remarkable formation of elastic fiber. The direction of the spindle-shaped, α-SMA-positive cells appeared relatively random at 3 months, but they were oriented in an orderly fashion around the circumference. On the other hand, the entire luminal surface was covered with a bold layer of elastic fiber that was very similar to lamina elastica interna. In addition, the anastomosis portion was infiltrated by a multilayered elastin fiber network. These changes indicated the adaptation process of the biotube to native artery. A longer implantation period may induce perfect regeneration of vascular tissue. These results suggested that the biotube is an excellent scaffold for regeneration of native tissues.

With regard to mechanical properties, before implantation the relationship between intraluminal pressure and external diameter in biotubes showed a "J"-shaped curve, similar to the native artery. The stiffness parameter (β), calculated from the relationship, is one of the indexes for compliance of blood vessels and indicates the mechanical property under physiological blood pressure, and was about 50, which was close to that of human coronary artery (39.8).[14] None of the biotubes ruptured even after 200 mmHg inner pressure, showing pressure resistance. In addition, periodic cycles of inflation and deflation of the biotubes were noted with repeated pressure loadings in their lumen, indicating pulsatile blood flow in the biotubes. In this study, little change in elongation ability of the biotube was observed before and after implantation, as it remained similar to that of the native artery. On the other hand, strength increased remarkably (by about 3×) after implantation, which may be due to the increased wall thickness (also about 3×) after implantation. Complete formation of layered elastic fibers in the entire wall may have induced elasticity similar to that of the native artery.

In vivo tissue-engineering approaches, which employed the host's inflammatory reaction to a foreign body to create a vascular graft *in vivo*, had been previously attempted by Campbell et al.[15] A relatively high patency rate of 67% was obtained at 4 months by layering mesothelium cells on the luminal surface of myofibroblast-walled tubes prepared in the peritoneal cavity of rats or rabbits. This is true even in the case of vascular grafts whose internal diameter is relatively large for small-caliber vascular grafts-3 mm in rats and 5 mm in rabbits. The concept of using the body as a reactor has also been reported for other types of grafts, for example, bone was constructed in an *in vivo* bioreactor.[16]

CONCLUSION

This study was the first to report long-term implantation of biotube vascular grafts for over 2 years. Vascular wall adaptation included a complete endothelial cell covering, a hierarchical vascular wall structure with circumferential orientation of collagen fibers and integrated cells, and elastic fibers on the luminal surface. This study is only suggestive, but it provides valuable insights to the field of regenerative medicine. To test the reliability of the results obtained in this study, another implantation study is currently being conducted in addition to further long-term implantation studies.

ACKNOWLEDGMENT

The authors thank Ms. Manami Sone for her participation in this study.

REFERENCES

1. Angelini GD, Newby AC. The future of saphenous vein as a coronary artery bypass conduit. Eur Heart J 1989;10:273–280.
2. Cameron A, Davis KB, Green G, Schaff HV. Coronary bypass surgery with internal-thoracic-artery grafts—Effects on survival over a 15-year period. N Eng J Med 1996;334:216–219.
3. Nakayama Y, Ishibashi-Ueda H, Takamazawa K. In vivo tissue-engineered small-caliber arterial graft prosthesis consisting of autologous tissue (biotube). Cell Transplant 2004;13:439–449.
4. Watanabe T, Kanda K, Ishibashi-Ueda H, Yaku H, Nakayama Y. Development of biotube vascular grafts incorporating cuffs for easy implantation. J Artif Organs 2007;10:10–15.
5. Watanabe T, Kanda K, Ishibashi-Ueda H, Yaku H, Nakayama Y. Autologous small-caliber "biotube" vascular grafts with argatroban loading: A histomorphological examination after implantation to rabbits. J Biomed Mater Res B: Appl Biomater 2010;92: 236–242.
6. Yamanami M, Yahata Y, Uechi M, Fujiwara M, Ishibashi-Ueda H, Kanda K, Watanabe T, Tajikawa T, Ohba K, Yaku H, Nakayama Y. Development of a completely autologous valved-conduit with the sinus of valsalva (biovalve) using in-body tissue architecture technology: A pilot study in pulmonary valve replacement in a beagle model. Circulation 2010;122(II Suppl):S100–S106.
7. Yamanami M, Yahata Y, Tajikawa T, Ohba K, Watanabe T, Kanda K, Yaku H, Nakayama Y. Preparation of in-vivo tissue-engineered valved conduit with the sinus of valsalva (type IV biovalve). J Artif Organs 2010;13:106–112.
8. Nakayama Y, Zhou YM, Ishibashi-Ueda H. Development of in vivo tissue-engineered autologous tissue-covered stents (biocovered stents). J Artif Organs 2007;10:171–176.
9. Langer R, Vacanti JP. Tissue engineering. Science 1993;206: 920–926.
10. Niklason LE, Gao J, Abbott WM, Hirschi KK, Hourser S, Marini R, Langer R. Functional arteries grown in vivo. Science 1999;284: 489–493.
11. Shinoka T, Imai Y, Ikada Y. Transplantation of a tissue engineered pulmonary artery. N Engl J Med 2001;344:532–533.
12. Iwakaki K, Kojima K, Kodama S, Paz AC, Chambers M, Umezu M, Vacanti CA. Bioengineered three-layered robust and elastic artery using hemodynamically-equivalent pulsatile bioreactor. Circulation 2008;118 (Suppl 1):S52–S57.
13. Kaushal S, Amiel GE, Guleserian KJ, Shapira OM, Perry T, Sutherland FW, Rabkin E, Moran AM, Schoen FJ, Atala A, Soker S, Bischoff J, Mayer JE, Jr. Functional small-diameter neovessels created using endothelial progenitor cells expanded ex vivo. Nat Med 2001;7: 1035–1040.
14. Hayashi K, Igarashi Y, Takamizawa K. Mechanical properties and hemodynamics in coronary arteries. In: Kitamura K, Abe H, Sagawa K, editors. New Approaches in Cardiac Mechanics. Tokyo: Japan Scientific Societies Press; 1986, pp 285–294.
15. Campbell JH, Efendy JL, Campbell GR. Novel vascular graft grown within recipient's own peritoneal cavity. Circ Res 1999;85: 1173–1178.
16. Stevens MM, Marini RP, Schaefer D, Aronson J, Langer R, Shastri VP. In vivo engineering of organs: The bone bioreactor. Proc Natl Acad Sci USA 2005;102:11450–11455.

Efficacy and Safety of Single versus Dual Antiplatelet Therapy for Coiling of Unruptured Aneurysms

Yusuke Nishikawa, MD,*† Tetsu Satow, MD, PhD,* Toshinori Takagi, MD,* Kenichi Murao, MD, PhD,‡ Susumu Miyamoto, MD, PhD,§ and Koji Iihara, MD, PhD*

Background: Although the efficacy of antiplatelet therapy for coiling of unruptured cerebral aneurysms has been reported, regimens for this therapy are not yet well established. The aim of this retrospective study was to analyze correlations among the modes of antiplatelet use, aneurysmal configuration, coiling methods, and complications to elucidate the optimal antiplatelet therapy for coiling. *Methods:* The study population comprised 154 patients with unruptured aneurysms who underwent coiling with antiplatelet therapy at our institution between 2001 and 2009. The patients were categorized by mode of antiplatelet therapy (single [n = 64] or dual [n = 90]), neck size (wide [n = 80] or narrow [n = 74]), and technique used (simple [n = 42] or adjunctive [n = 112]). The incidences of hemorrhagic/ischemic complications and abnormalities on postprocedural diffusion-weighted magnetic resonance imaging (DWI) in each group were statistically assessed. *Results:* Hemorrhagic complications occurred in 1 case (1.5%) with single antiplatelet therapy and in 2 cases (2.2%) with dual antiplatelet therapy. Symptomatic ischemic complications occurred in 5 cases (7.8%) with single therapy and in 4 cases (4.4%) with dual therapy. Abnormalities were detected by DWI in 27 cases (42%) with single therapy and in 31 cases (34%) with dual therapy. No significant difference was found between modes of antiplatelet therapy even when the technique used was taken into account. In cases of wide neck, however, there were significant differences in the rate of symptomatic ischemic complications (single, 21.7%; dual, 3.5%; $P = .014$) and DWI abnormalities (single, 37.8%; dual, 20.9%; $P = .048$). *Conclusion:* Our data suggest that dual antiplatelet therapy may better prevent ischemic complications from coiling for wide-necked aneurysms compared with single antiplatelet therapy. **Key Words:** Coil embolization—antiplatelet therapy—neck width—thromboembolic complication.

Coil embolization for intracranial aneurysms has become a common technique with the development of devices and adjunctive techniques, such as balloon-assisted and double-catheter techniques. Thromboembolic events are the most feared complication of coil embolization, with a frequency of 5.52%-9%.[1-3] The use of antiplatelet drugs during the periprocedural period has been proposed to decrease the risk of this unfavorable complication, and previous studies have reported its efficacy.[4-13] None of those studies specified the optimal dose and mode (single or dual) for antiplatelet therapy, however, particularly in relation to the use of adjunctive

From the *Department of Neurosurgery, National Cerebral and Cardiovascular Center, Osaka, Japan; †Department of Neurosurgery, Nagoya City University, Nagoya, Japan; ‡Department of Neuroendovascular Therapy, Shiroyama Hospital, Osaka, Japan; and §Department of Neurosurgery, Kyoto University, Kyoto, Japan.

Received October 17, 2011; revision received February 7, 2012; accepted February 11, 2012.

Address correspondence to Yusuke Nishikawa, MD, Department of Neurosurgery, Nagoya City University School of Medicine, 1 Kawasumi, Mizuho-cho, Mizuho-ku, Nagoya 467-8602, Japan. E-mail: yusuken@med.nagoya-cu.ac.jp.

1052-3057/$ - see front matter

doi:10.1016/j.jstrokecerebrovasdis.2012.02.008

techniques and aneurysmal configuration (ie, neck size) in a large series.

In the present study, patients who underwent coil embolization for unruptured cerebral aneurysm at our institution were examined retrospectively to elucidate the optimal antiplatelet therapy, which decreases the risk of ischemic complications while minimizing hemorrhagic adverse events.

Methods

Patient Population

This study was a retrospective analysis of 154 consecutive adult patients undergoing elective coil embolization of 157 intracranial saccular aneurysms between June 2001 and June 2009 at our institution. Exclusion criteria were partially thrombosed aneurysm, fusiform aneurysm treated by parent artery occlusion, no antiplatelet therapy, combination of oral anticoagulant therapies, retreatment, and stent-assisted cases.

All cases were classified by the technique used (simple or adjunctive) and the mode of antiplatelet therapy (single or dual), resulting in 4 subgroups: S1, simple technique with single antiplatelet therapy; S2, simple technique with dual antiplatelet therapy; A1, adjunctive technique with single antiplatelet therapy; and A2, adjunctive technique with dual antiplatelet therapy. Subjects were also classified by neck width (wide, ≥4 mm; narrow, <4 mm), in accordance with the report by Murayama et al,[14] and by the mode of antiplatelet therapy into another 4 subgroups: N1, narrow neck with single antiplatelet therapy; N2, narrow neck with dual antiplatelet therapy; W1, wide neck with single antiplatelet therapy; and W2, wide neck with dual antiplatelet therapy. In cases with multiple aneurysms, the aneurysm with wider neck size was counted for categorization between narrow and wide subgroups.

Antiplatelet Therapy

Administration of antiplatelet drugs was started at least 4 days before the procedure. Single agent therapy was provided with aspirin 81-200 mg/day. For dual therapy, cilostazol 100-200 mg/day, ticlopizine 100-200 mg/day, or clopidogrel 75 mg/day was added to aspirin. In the dual therapy regimens, aspirin was the first-line drug, with cilostazol or thienopyridine (ticlopidine/clopidogrel) used as an adjuvant. Aspirin/cilostazol therapy was more common than aspirin/thienopyridine therapy (68% vs 31%). In terms of the duration of antiplatelet use, administration was completed within 1-6 months after the procedure in the single therapy group. In the dual therapy group, antiplatelet drugs were reduced to one drug (aspirin in most cases) at 1 week to 3 months after the procedure, and administration was completed within the subsequent 3-6 months.

Procedure

The procedures were performed using transfemoral arterial access in a dedicated biplane neuroangiography suite (BV-3000; Philips, Best, The Netherlands), under general anesthesia after obtaining informed consent from the patient and family members. All procedures in this series were performed by 2 neuroendovascular therapists (K.M. and T.S.).

The endovascular procedures were performed after endotracheally induced general anesthesia. Anticoagulation was provided by heparin (initial dose of 4000 IU) after arterial access was obtained through the femoral artery. Coil insertion was started after confirmation of activated clotting time >250 seconds, with continuous administration of heparin to maintain activated clotting time at ~250-300 seconds. The neck remodeling technique was performed if necessary, and HyperForm or HyperGlide (ev3; Plymouth, MN) balloon catheters were used. Only bare platinum coils were placed in the sac, with the exception of 2 cases in which Matrix 2 coils (Boston Scientific, Fremont, CA) were used. After completion of coil placement, systemic heparinization was stopped but not reversed, and hemostasis at the vascular access was secured by Angioseal (St Jude Medical, Austin, TX) in most cases. Patients were transferred to a neurosurgical intensive care unit and received intravenous argatroban (120 mg/day) for 2 days.

Evaluation of Diffusion-Weighted MRI

Diffusion-weighted MRI (DWI) was performed 2-5 days after the procedure using a 1.5-T system (Magnetom Vision; Siemens, Erlangen, Germany) with a multisection, single-shot, spin-echo planar imaging sequence. Diffusion gradients were applied in each of the x, y, and z directions with 2 b values (0 and 1000 s/mm^2). Imaging parameters were as follows: echo time, 100 ms; field of view, 23 cm; matrix, 96 × 128; section thickness, 4 mm; and intersection gap, 2 mm. Conventional spin-echo magnetic resonance imaging (MRI) was also performed at each examination under T1- and T2-weighted conditions and with a fluid-attenuated inversion recovery sequence. All MRI images were reviewed by neuroradiologists who were blinded to the clinical information. When abnormalities were detected on DWI, the locations were recorded.

Statistical Analysis

Analyses were performed using JMP version 8.0 (SAS Institute, Cary, NC). Statistical significance for intergroup differences was assessed using the z test for categorical variables and the Mann-Whitney U test for continuous variables. The incidence of symptomatic ischemic complication, DWI abnormalities, and hemorrhagic complications were calculated, and statistical analyses were performed among subgroups sorted by neck size and

Table 1. *Comparison of narrow-necked and wide-necked cases (n = 154)*

	Narrow neck (n = 74; 48.1%)	Wide neck (n = 80; 51.9%)	*P* value
Adjunctive technique, n (%)	48 (64.9)	64 (80.0)	.035
Symptomatic ischemic complications, n (%)	2 (2.7)	7 (8.8)	NS
DWI abnormality, n (%)	21 (28.4)	37 (46.3)	.022

Abbreviation: NS, not significant.

A population test was performed. The adjunctive technique was significantly used when the aneurysmal neck was wide. There was an increase in postprocedural DWI abnormalities in wide-necked cases despite the statistically significant difference.

mode of antiplatelet therapy (W1, W2, N1, and N2) or technique used and mode of antiplatelet therapy (S1, S2, A1, and A2). Furthermore, symptomatic ischemic complications and DWI abnormalities were tested using age, sex, mode of antiplatelet therapy, adjunctive technique, neck size, and aneurysmal location with multivariate analysis by logistic regression. *P* values <.05 were considered to indicate a significant difference.

Results

The mean age of the study patients was 58.8 years (range, 27-80 years), and 76% (117 of 154) of patients were female. The mean maximum aneurysm diameter was 7.38 ± 2.91 mm, with a median size of 6.70 mm (range, 3.2-19.6 mm). The mean neck width was 4.20 ± 1.46 mm, with a median size of 4.0 mm (range, 1.82-10.2 mm). Of the aneurysms treated, 92 involved the internal cerebral artery (including posterior communicating artery aneurysms), 27 were at the basilar bifurcation, 15 involved the anterior cerebral artery (including the anterior communicating artery), 11 involved the basilar artery/superior cerebellar artery, 1 involved the middle cerebral artery, and 11 involved other posterior fossa sites. Multiple aneurysms were present in 3 cases. A total of 42 cases were treated using the simple technique (only one microcatheter used for coiling), and the remaining 112 cases were treated using an adjunctive technique (balloon-assist, double-catheter, or both).

Symptomatic ischemic complications were seen in 9 cases (5.8%), including 3 with transient ischemic attack (TIA). Onset of all TIAs occurred within 24 hours after the procedure. The remaining 6 symptomatic ischemic complications were nondisabling stroke (modified Rankin scale score, 0-2). DWI abnormalities were observed in 58 cases (37.7%), with 50 (32.5%) not associated with any symptoms, representing so-called "silent ischemia." One case with TIA exhibited no DWI abnormalities. Hemorrhagic complications occurred in 3 cases (1.9%), including 1 patient with intracranial hemorrhage and 2 patients with extracranial bleeding (one with groin hematoma and the other with bleeding from a gastric ulcer). No intraprocedural bleeding occurred. Dual antiplatelet therapy had been administered to 2 of the 3 patients who sustained hemorrhage.

Categorization by Technique and Mode of Antiplatelet Therapy

There were 20 cases (13%) in the S1 subgroup, 22 (14%) in the S2 subgroup, 44 (29%) in the A1 subgroup, and 68 (44%) in the A2 subgroup. The distribution of cases with symptomatic ischemia was 3 (15%) in S1, 1 (4.5%) in S2, 2 (4.5%) in A1, and 3 (4.4%) in A2. No significant differences were found between S1 and S2 (*P* = .22) or between A1 and A2 (*P* = .66).

DWI abnormalities were observed in 10 cases (50%) in S1, 5 (22.7%) in S2, 17 (38.6%) in A1, and 26 (38.2%) in A2. No significant differences were seen between S1 and S2 (*P* = .06) or between A1 and A2 (*P* = .91) in this cohort.

Categorization by Neck Width and Mode of Antiplatelet Therapy

A narrow neck was present in 74 cases; a wide neck, in 80 cases. A significant correlation was noted between neck size and DWI abnormalities (*P* = .02) (Table 1). According to categorization by neck width and mode of

Table 2. *Comparison of single and dual antiplatelet therapy in narrow-necked cases (n = 74)*

	N1 (n = 41; 55.4%)	N2 (n = 33; 44.6%)	*P* value
Adjunctive technique, n (%)	27 (65.8)	21 (63.6)	NS
Symptomatic ischemic complications, n (%)	1 (2.4)	1 (3.0)	NS
DWI abnormality, n (%)	13 (31.7)	8 (24.2)	NS

Abbreviations: NS, not significant; N1, narrow neck with single antiplatelet therapy; N2, narrow neck with dual antiplatelet therapy.

Comparisons were made between N1 and N2, and a population test was performed.

Table 3. *Comparison of single and dual antiplatelet therapy in wide-necked cases (n = 80)*

	W1 (n = 23; 28.8%)	W2 (n = 57; 71.3%)	*P* value
Adjunctive technique, n (%)	17 (73.9)	47 (82.5)	NS
Symptomatic ischemic complications, n (%)	5 (21.7)	2 (3.5)	.014
DWI abnormality, n (%)	14 (60.9)	23 (40.4)	.047

Abbreviations: NS, not significant; W1, wide neck with single antiplatelet therapy; W2, wide neck with dual antiplatelet therapy.
Comparisons were made between W1 and W2, and a population test was performed. Significant differences in the occurrence of symptomatic ischemic events and DWI abnormalities were seen between W1 and W2.

antiplatelet therapy, the subgroup distribution was 41 (27%) for N1, 33 (21%) for N2, 23 (15%) for W1, and 57 (37%) for W2. The ratio of adjunctive technique was not significant in any group (N1 and N2, $P = .340$; W1 and W2, $P = .289$). The distribution of patients with symptomatic ischemia was 1 (2.4%) in N1, 1 (3.0%) in N2, 5 (21.7%) in W1, and 2 (3.5%) in W2. A significant difference in the occurrence of symptomatic ischemic events was apparent between W1 and W2 (odds ratio [OR], 0.131; 95% confidence interval [CI], 0.023-0.734; $P = .014$), whereas the comparison of N1 and N2 revealed no significant difference ($P = .714$) (Tables 2 and 3; Fig 1).

The subgroup distribution of cases with DWI abnormalities was 13 (31.7%) in N1, 8 (24.2%) in N2, 14 (60.9%) in W1, and 23 (40.4%) in W2. There as a significant difference between W1 and W2 ($P = .047$). The ratio of new lesions detected by DWI was significantly decreased in wide neck cases using dual antiplatelet therapy (Tables 2 and 3).

The associations of DWI-detected lesions with age, sex, antiplatelet therapy, adjunctive technique, neck size, and relationship with the parent artery were tested with multivariate analysis using logistic regression (Table 4). Analysis identified neck width as a factor independently correlated with the presence of DWI abnormalities ($P = .015$), and showed that dual antiplatelet therapy was likely to reduce the rate of DWI abnormalities ($P = .056$).

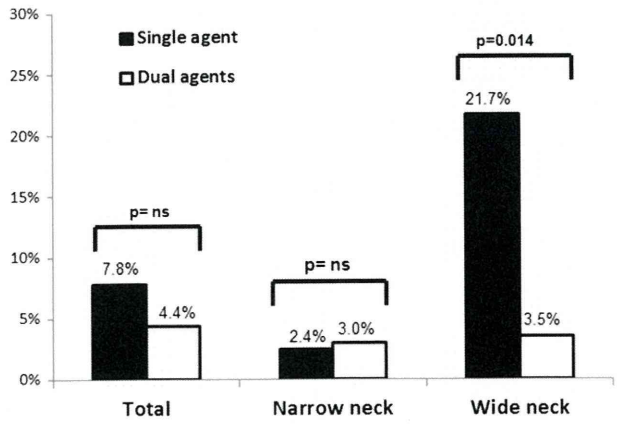

Figure 1. *Bar graph showing the occurrence of symptomatic ischemic events. A significant difference in the occurrence of symptomatic ischemic events was apparent between W1 and W2 (OR, 0.131; 95% CI, 0.023-0.734; P = .014), whereas the comparison between N1 and N2 demonstrated no significant difference.*

Discussion

Thromboembolism is the most common complication associated with coil embolization. The rate of this fearful complication ranged from 5.52% to 9% of cases in several previous clinical series.[1-3] Several recent reports have described the efficacy of periprocedural administration of antiplatelet drugs in preventing thromboembolism associated with coil embolization. Yamada et al[4] reported a reduction in the thromboembolic event rate among patients who received antiplatelet therapy either after or both before and after endovascular treatment. Layton et al[6] demonstrated the efficacy of periprocedural antiplatelet therapy and differentiated antiplatelet regimens into 3 groups: aspirin, clopidogrel, and a combination of the two. Although Layton et al concluded that the use of clopidogrel (either alone or in combination with aspirin) was the only preprocedural antiplatelet factor that showed any significant effect on local thrombus formation or symptomatic thromboembolic complications, the number of cases treated with antiplatelet drugs was small, and correlations between antiplatelet drugs and use of the balloon-assist technique were not assessed in terms of thromboembolism. No previous studies have investigated established antiplatelet regimens, particularly regarding the mode of antiplatelet drugs (single or dual) and the duration of antiplatelet therapy.

This retrospective study collected data for coil embolization of unruptured cerebral aneurysms in which periprocedural antiplatelet therapy was administered. According to the literature, factors likely associated with thromboembolism include aneurysm neck width and the use of an adjunctive technique.[5,7,15] We focused on these factors and on the antiplatelet regimen to evaluate correlations among them and with the incidence of periprocedural complications to elucidate the optimal antiplatelet therapy, with the aim of preventing thromboemobolic events without increasing hemorrhagic complications.

We added abnormalities on DWI, the imaging modality providing the most sensitive detection of early and small ischemic lesions, as one of the study endpoints because of the anticipated low rate of symptomatic ischemic

Table 4. *Results of logistic regression analysis for abnormalities identified on DWI (n = 154)*

	Profile	OR (95% CI)	*P* value
Demographics			
Male, n (%)	37 (24.0)	0.790	NS
Age, years	58.8 ± 10.0	2.263 (0.37-17.4)	NS
Aneurysmal factors			
Neck, mm	4.19 ± 1.46	20.66 (2.11-250.5)	.015
Terminal type/side wall type, n	68/86	2.006	NS
Procedure-related factors			
Single/dual agents, n	64/90	2.008	.056
Simple/adjunctive technique, n	42/112	1.072	NS

Abbreviation: NS, not significant.

complications during coiling in patients receiving antiplatelet therapy. As to the combination of antiplatelet agents for dual therapy, aspirin was the first choice in all cases. The concomitant use of cilostazol and ticlopidine/clopidogrel was absent in this study, due mainly to medicofinancial factors.

There were no definite regimen whether single or dual antiplatelet therapy was applied in each case in this retrospective study; however, dual antiplatelet agents were used preferentially in cases involving the balloon-assist technique. This preference was based on data from our previous study showing an increased incidence of silent ischemia when balloon catheters were used.[5,11]

Therefore, we first investigated the efficacy of dual antiplatelet therapy over single antiplatelet therapy when an adjunctive technique was used, and found no statistically significant difference. This finding supports the results of Brooks et al[9] and Albayram et al,[16] indicating that the balloon-assist technique itself is not a risk factor for thromboembolism.

On the other hand, significant differences in both the occurrence of symptomatic ischemic complications and the detection of new lesions on DWI when the mode of antiplatelet therapy (single or dual) was sorted by neck width (Table 3 and Fig 1). In cases with a wide-necked aneurysm, dual antiplatelet therapy decreased both symptomatic and asymptomatic ischemia. A possible mechanism underlying the increased ischemic complications in wide-necked cases is the increased coil–parent artery interface, as supported by Klötzsch et al.[17] This idea has been advanced in previous studies[4-13]; however, the present study is the first to demonstrate the efficacy of dual antiplatelet therapy over single antiplatelet therapy for aneurysmal coil embolization in wide-necked cases.

Cilostazol, an inhibitor of phosphodiesterase 3,[18] was shown to have superior efficacy and safety over aspirin in the Cilostazol Stroke Prevention Study 2.[19] The preferential use of cilostazol as an adjuvant to aspirin in the present was based on results from the Trial of Cilostazol in Symptomatic Intracranial Arterial Stenosis, which proved that the rate of hemorrhagic complications did not increase with the addition of cilostazol to aspirin,[20] and the fact that clopidogrel was unavailable in Japan until 2006.

The incidence of hemorrhagic complications was low in our series. Possible factors contributing to this finding may be the preferential use of cilostazol and the relatively short duration of antiplatelet use, which has been associated with a low risk of hemorrhagic events in several studies.[4,21,22]

The concept of using neck width, a parameter that can be easily measured before the procedure, to determine the mode of antiplatelet therapy is simple and comprehensible. A prospective, large-volume study is needed to verify whether the single antiplatelet therapy is sufficient for cases with a narrow neck, which seems preferable in terms of drug compliance and medicofinancial perspectives.

This study has some limitations. First, this was a retrospective study, and the dose and the mode of antiplatelet therapies (single or dual) might have been biased. Second, the number of study participants was insufficient to provide further information especially regarding the optimal period of antiplatelet therapy, which is another keystone for establishing optimal regimens. Further prospective evaluation is warranted to determine the optimal dose, duration, and tapering schedule for antiplatelet drugs. A prospective randomized trial will identify the optimal antiplatelet therapy for coiling of unruptured aneurysms.

Conclusion

Periprocedural dual antiplatelet therapy for coiling of unruptured cerebral aneurysms may prevent the incidence of both symptomatic ischemic complication and DWI abnormalities for wide-necked aneurysms compared with single antiplatelet therapy. Conversely, the mere use of adjunctive techniques might not be a sufficient indication for the use of dual antiplatelet therapy.

References

1. Park HK, Horowitz M, Jungreis C, et al. Periprocedural morbidity and mortality associated with endovascular

treatment of intracranial aneurysms. AJNR Am J Neuroradiol 2005;26:506-514.
2. Im S-H, Han MH, Kwon O-K, et al. Endovascular coil embolization of 435 small asymptomatic unruptured intracranial aneurysms: Procedural morbidity and patient outcome. AJNR Am J Neuroradiol 2009;30:79-84.
3. Gallas S, Drouineau J, Gabrillargues J, et al. Feasibility, procedural morbidity and mortality, and long-term follow-up of endovascular treatment of 321 unruptured aneurysms. AJNR Am J Neuroradiol 2008;29:63-68.
4. Yamada NK, Cross DT III, Pilgram TK, et al. Effect of antiplatelet therapy on thromboembolic complications of elective coil embolization of cerebral aneurysms. AJNR Am J Neuroradiol 2007;28:1778-1782.
5. Soeda A, Sakai N, Sakai H, et al. Thromboembolic events associated with Guglielmi detachable coil embolization of asymptomatic cerebral aneurysms: Evaluation of 66 consecutive cases with use of diffusion-weighted MR imaging. AJNR Am J Neuroradiol 2003;24:127-132.
6. Layton KF, Cloft HJ, Gray LA, et al. Balloon-assisted coiling of intracranial aneurysms: Evaluation of local thrombus formation and symptomatic thromboembolic complications. AJNR Am J Neuroradiol 2007;28:1172-1175.
7. Rordorf G, Bellon RJ Jr, Farkas J, et al. Silent thromboembolic events associated with the treatment of unruptured cerebral aneurysms by use of Guglielmi detachable coils: prospective study applying diffusion-weighted imaging. AJNR Am J Neuroradiol 2001;22:5-10.
8. Koebbe CJ, Veznedaroglu E, Jabbour P, et al. Endovascular management of intracranial aneurysms: Current experience and future advances. Neurosurgery 2006;59. S3-93-102.
9. Brooks NP, Turk AS, Niemann DB, et al. Frequency of thromboembolic events associated with endovascular aneurysm treatment: Retrospective case series. J Neurosurg 2008;108:1095-1100.
10. Katsaridis V, Papagiannaki C, Violaris C. Guglielmi detachable coils versus matrix coils: a comparison of the immediate posttreatment results of the embolization of 364 cerebral aneurysms in 307 patients. A single-center, single-surgeon experience. AJNR Am J Neuroradiol 2006; 27:1841-1848.
11. Soeda A, Sakai N, Murao K, et al. Thromboembolic events associated with Guglielmi detachable coil embolization with use of diffusion-weighted MR imaging, part II: Detection of the microemboli proximal to cerebral aneurysm. AJNR Am J Neuroradiol 2003;24:2035-2038.
12. Qureshi AI, Mohammad Y, Yahia AM, et al. Ischemic events associated with unruptured intracranial aneurysms: Multicenter clinical study and review of the literature. Neurosurgery 2000;46:282-290.
13. Sluzewski M, van Rooij WL, Beute GN, et al. Balloon-assisted coil embolization of intracranial aneurysms: Incidence, complications, and angiography results. J Neurosurg 2006;105:396-399.
14. Murayama Y, Nien YL, Duckwiler G, et al. Guglielmi detachable coil embolization of cerebral aneurysms: 11 years' experience. J Neurosurg 2003;98:959-966.
15. van Rooij WJ, Sluzewski M, Beute GN, et al. Procedural complications of coiling of ruptured intracranial aneurysms: incidence and risk factors in a consecutive series of 681 patients. AJNR Am J Neuroradiol 2006;27. 1498-1450.
16. Albayram S, Selcuk H, Kara B, et al. Thromboembolic events associated with balloon-assisted coil embolization: Evaluation with diffusion-weighted MR imaging. AJNR Am J Neuroradiol 2004;25: 1768-1777.
17. Klötzsch C, Nahser HC, Henkes H, et al. Detection of microemboli distal to cerebral aneurysms before and after therapeutic embolization. AJNR Am J Neuroradiol 1998;19:1315-1318.
18. Sudo T, Tachibana K, Toga K, et al. Potent effects of novel anti-platelet aggregatory cilostamide analogues on recombinant cyclic nucleotide phosphodiesterase isozyme activity. Biochem Pharmacol 2000;59:347-356.
19. Shinohara Y, Katayama Y, Uchiyama S, et al. Cilostazol for Prevention of Secondary Stroke (CSPS 2): An aspirin-controlled, double-blind, randomized non-inferiority trial. Lancet Neurol 2010;9:959-968.
20. Kwon SU, Cho YJ, Koo JS, et al. Cilostazol prevents the progression of symptomatic intracranial arterial stenosis: The multicenter double-blind placebo-controlled trial of cilostazol in symptomatic intracranial arterial stenosis. Stroke 2005;36:782-786.
21. Bhatt DL, Fox KAA, Hacke W, et al. Clopidogrel and aspirin versus aspirin alone for the prevention of atherothrombotic events. N Engl J Med 2006;354: 1706-1717.
22. Gyojun H, Chulkyu J, Sukh QP, et al. Thromboembolic complications of elective coil embolization of unruptured aneurysms: The effect of oral antiplatelet preparation on periprocedural thromboembolic complication. Neurosurgery 2010;67:743-748.

頭頚部動脈瘤治療のための微細多孔薄膜カバードステントの開発：微細孔設計のための生体外実験

紅林芳嘉[1,3]，中川雄太[2,3]，田地川勉[1]，大場謙吉[1]，中山泰秀[3]，西正吾[4]
[1]関西大学　システム理工学部　機械工学科
[2]関西大学　大学院　理工学研究科
[3]国立循環器病研究センター　生体医工学部
[4]札幌東徳洲会病院　脳神経外科

Development of microporous covered stents for cranial aneurysm treatment : in vitro flow experiment for pore design

Yoshihiro Kurebayashi[1,3], Yuta Nakagawa[2,3], Tsutomu Tajikawa[1], Kenkichi Ohba[1], Yasuhide Nakayama[3], Syogo Nishi[4]
[1]Department of Mechanical Engineering,Kansai University,Osaka,Japan
[2]Department of Science and Engineering, Graduate school of Kansai University,Osaka,Japan
[3]Department of Biomedical Engineering,National Cerebral and Cardiovascular Center,Osaka,Japan
[4]Department of Neurosurgery, Sapporo Higashi-Tokushukai Hospital, Sapporo, Japan

Abstract: We have been developing microporous covered stents for aneurysm treatment. In animal experiment , an increasing in total opening ratio of micropores from 12.6% to 23.6% allowed inhibition of intimal hyperplasia in addition to complete embolization of aneurysm. Therefore , it is expected that thinner intima will be brought by further increasing in the opening ratio. However, in this case incomplete embolization may be occurred. In this study, we investigated the influence of the pore size and its opening ratio on flow pattern and rate by using an in vitro flow circuit with aneurysm model for optimization of the pore design. Flow patterns inside the aneurysm models were visualized under various Reynolds number of the parent vessel between 170 and 950 in steady flow. The dead water region was observed at the top of the aneurysm model with certain microporous films (d = 300 ~ 500μm) , which may lead ideal micropores design.

Keywords: Microporous covered stents , In vitro experiments , Flow visualization

1. Introduction　脳動脈瘤の治療として，瘤の開口部をクリップで挟む外科的治療と，瘤内にコイルを詰めて塞栓させる血管内治療が行われている.しかし，いずれの方法においても大瘤や大開口瘤の治療は困難な場合が多い.そこで我々は，それらの動脈瘤でも低侵襲で簡便かつ確実に治療できるデバイスとして，図 1 に示す微細多孔薄膜カバードステントの開発を行っている.本カバードステントの構造的特徴として，ステント基材が薄いフィルム内に埋め込まれ，そのフィルムに微細孔(直径 100～300μm)が一様にあけられている.

これまで，動物実験において微細孔の開口率を12.6%から 23.6%に増加させても，完全な動脈瘤の塞栓が維持され，内膜肥厚が抑制されることを報告した.さらに開口率を増やすことで早期の内膜化が期待できるが，瘤の塞栓が不完全となることが懸念される.そこで，本研究では微細孔の設計最適化を目的として，孔径と密度が瘤内流れに及ぼす影響を可視化実験により調べた.

2. Methods　生体外模擬循環回路の概略図を図 2 に示す.定常流を動脈瘤モデルに流入させ，瘤内流れの可視化を行った.実験に用いた動脈瘤モデルを図 3 に示す.瘤内の二次流れの影響を無視し，現象を簡単化するためモデルは二次元にし，アクリルを切削して作製した.親血管は，高さ b [mm]と式(1)で示される水力平均直径が治療対象の血管径と一致するように一辺 b の正方断面とし，b=3mm あるいは 5mm とした.ここで s は管の周長，A は管断面積である.

$$D = \frac{4A}{s} \qquad (1)$$

動脈瘤モデルに設置する微細多孔膜を図 4 に示す.微細多孔膜はポリイミドフィルム(厚さ 25μm)にエキシマレーザーを用いて，孔径 d [mm]と開口率 A* [%]を系統的に変化させた円孔を開けて作製した.作動流体にはヒト血液と動粘度がほぼ等しい 45wt%グリセリン水溶液(密度 1090kg/m^3,動粘度ν =4.03×10^{-6}m^2/s)を用いた.流入条件は式(2)で定義される Reynolds数Re をヒト脳動脈内流速と同じ Re = 170～950 とした.ここで u は親血管平均流速 , D は親血管の水力平均直径である.

$$\mathrm{Re} = \frac{uD}{\nu} \qquad (2)$$

可視化には注入流跡法を用い，図 2 に示すように Ar$^+$レーザー(波長 514.5nm)を光源としたレーザーシートをモデルのほぼ中央断面に照射し，デジタルカメラでモデルの正面から露光時間を調節しながら撮影した.トレーサー粒子はフライアッシュ(密度 1950kg/m^3,平均粒径 20μm)を用いた.

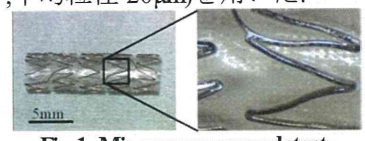

Fig. 1 Microporous covered stent.

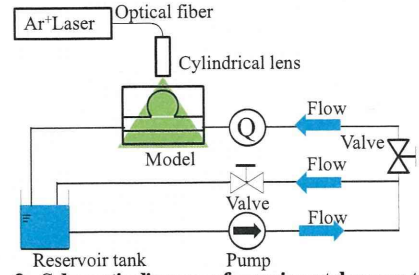

Fig. 2 Schematic diagram of experimental apparatus.

3. Results and Considerations b=5mmとして作製したモデルについて主に説明を行う.多孔薄膜を留置しない瘤内の流れを図5に示す.瘤開口部の流体が主流のせん断を受けて流動することで瘤内は回転循環流れとなった.このような流れを主流誘起型と定義した.

微細多孔膜をモデル開口部に留置した場合の瘤内流れの一例 (d = 400μm, A* = 60%)を図6に示す.低Re数領域では,留置しなかった場合と循環流の回転方向が逆であった.微細多孔膜を瘤の開口部に留置することで瘤内流れが主流と分断され,主流の圧力損失が駆動力となって瘤内に流れが起こったと考えられる.この流れを圧力損失型の流れと定義した.またRe数を増加させると,瘤内流れが圧力損失型から主流誘起型へと遷移し,瘤内流れのパターンは孔径 d,開口率 A*に関わらず,以下の4つに分類できた.各実験条件で得られたパターンをマッピングした結果を図7に示す.

(A)開口部の中央を渦中心とする圧力損失型
(B)渦中心が下流側に寄った圧力損失型
(C)圧力損失型と主流誘起型が共存する流れ
(D)主流誘起型が支配的な流れ

瘤内の流れは,孔径 200μm以下では,Re数に関わらずパターン A となり,流速の増加に伴い回転速度が増加した.一方,孔径300μm以上では,開口率を40%以上に増加させると, Re 数の増加に伴い,パターンAからパターン Dへ流れが遷移した.また,その遷移途中のパターンBとパターンCにおいて,瘤内上部に流れの澱みが観察され,塞栓に有利と考えられた.フローパターンの遷移は大孔径かつ大開口率ほど,低いRe数で起こった.

また,図7(a)と(b)を比較すると,b=5mmおよび3mmのフローパターンマップに大きな差異は認められない.よって, 今回実験したモデルの寸法では,瘤内流れのパターンはモデル寸法の影響を受けておらず,留置する多孔薄膜の孔径と開口率の大きさに依存していることが分かった.

4. Conclusions 二次元動脈瘤モデルに孔径および開口率の異なる多孔薄膜を留置し,定常流下での瘤内流れの様子を可視化実験により調べた結果,以下のことが分かった.

・今回の実験条件の範囲内では,モデルの寸法によらず,主流の Reynolds 数が増加するに従い,圧力損失型から,主流誘起型のフローパターンへ遷移した.また,留置する多孔薄膜が大孔径かつ大開口率ほど,低いReynolds数で遷移した.

・瘤内流れパターンの遷移過程において,瘤内上部で流れの澱みが起こり,動脈瘤の塞栓に有利であると考えられた.

留置する多孔薄膜の孔径および開口率を変化させることで瘤内の流れパターンを大きく変化させることができ,瘤内の流れを澱ませることが可能であった.今後,血液凝固実験ならびに動物実験による検証を進めていく予定である.

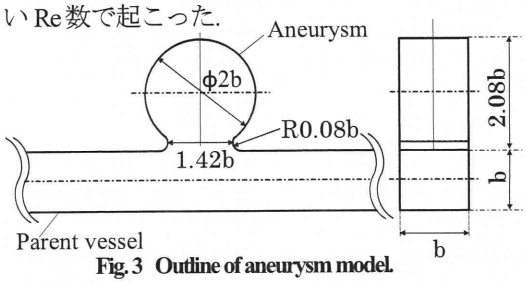

Fig.3 Outline of aneurysm model.

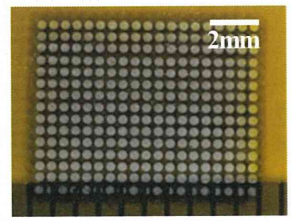

Fig.4 Microporous film.

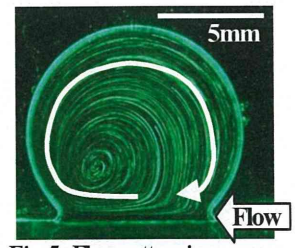

Fig.5 Flow pattern in aneurysm without film.

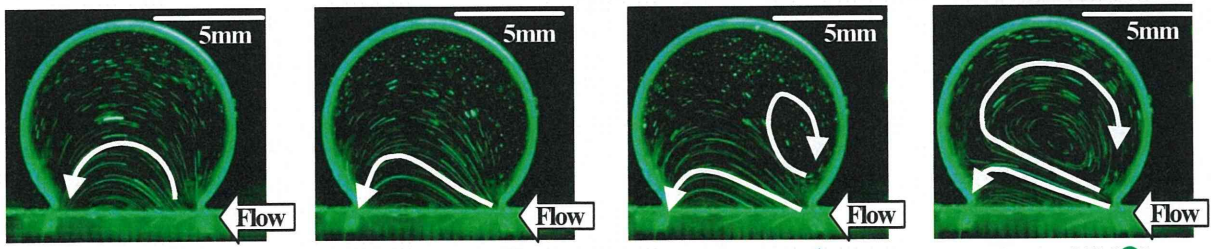

(A) Re=170 [○] (B) Re=290 [■] (C) Re=580 [▲] (D) Re=950 [●]

Fig.6 Flow patterns in intra-aneurysm model with a microporous film (d=400μm,A*=60%).

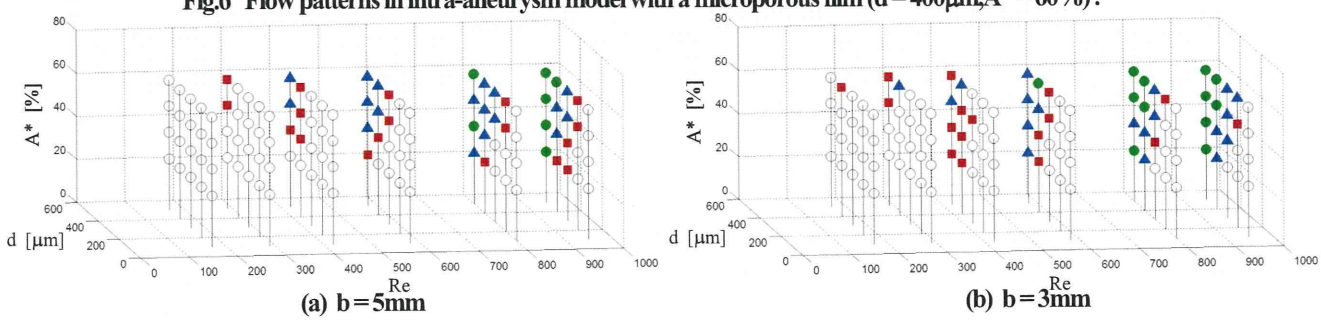

(a) b=5mm (b) b=3mm

Fig.7 Flow patterns maps.